INT. J. REMOTE SENSING, 2001, VOL. 22, NO. 5, 889–894

Fractality in broken clouds and the scan geometry of new satellite-borne infrared sensors

C. PIETRAPERTOSA, V. CUOMO, N. PERGOLA

Instituto di Metodologie Avanzate per Analisi Ambientale del CNR, Tito Scalo, Potenza, Italy

C. SERIO, V. TRAMUTOLI

Dipartimento di Ingegneria e Fisica dell'Ambiente, Universitá della Basilicata, Potenza, Italy

and H. SHIMODA

Tokay University, Research and Information Center, Tokyo, Japan

(Received 17 February 2000; in final form 31 August 2000)

Abstract. Cloud scenes observed by the Advanced Visible and Near-Infrared Radiometer on board the Japanese polar platform Advanced Earth Observing Satellite have been analysed to check the validity of power laws extending from the length scale of a few metres to several kilometers. The kind of scaling law we have investigated pertains to cloud morphology and may have important implications for the design of the scan geometry of new satellite-borne infrared sensors aimed at improving the density of clear soundings in frontal systems.

1. Introduction

Since Mandelbrot (1982) claimed the ubiquity of fractality in nature, cloud morphology has been the subject of many studies which have attempted to show its fractal nature (Lovejoy 1982, Parker *et al.* 1986, Lovejoy *et al.* 1987, Yano and Takeuchi 1987, Duroure and Guillemet 1990). It has been suggested that atmospheric convection itself tends to produce a particular type of cloud organization that, especially in frontal regions, is scale invariant, that is the spatial cloud patterns have no intrinsic length scale (Weger *et al.* 1992, 1993, Zhu *et al.* 1992). However, scale invariance may break at some particular scale so that the question still remains of the range of scales over which clouds behave as fractal objects. Analysing AVHRR (Advanced Very High Resolution Radiometer) cloud patterns in frontal systems Serio and Tramutoli (1995) evidenced a power law structure for the variance spectrum which again is a sign of fractality at least down to 1000 m scale, that is the spatial resolution of AVHRR. In this Letter, it will be shown that scaling laws characterize cloud morphology down to spatial scales of a few metres, a result which has not been reported previously.

Frontal systems and more in general patterns of broken clouds are interesting in

International Journal of Remote Sensing
ISSN 0143-1161 print/ISSN 1366-5901 online © 2001 Taylor & Francis Ltd
http://www.tandf.co.uk/journals
DOI: 10.1080/01431160010013801

the context of applications of remote sensing from space. It is now commonly recognized that Numerical Weather Prediction and, more in general, the remote sensing of land surface properties would improve in quality if the density of soundings in clear sky conditions increased by 1–2 orders of magnitude over the current satellite-based systems. Because of that the quest of smaller field-of-view for infrared sounders is characterizing the design of new and modern satellite infrared sensors. May fractality of clouds be put at work, to some extent, to assist the design of the scan geometry of new infrared sensors? Frontal systems are characterized by broken clouds so that we could gain insight into designing the scan geometry of sensors if we were able to model the density and size of holes in cloud systems in a mathematical framework.

It is a result due to van der Ziel (1950) that if a generic stochastic process is characterized by a power law spectra (frequency or wavenumber domain) then the same process is governed by a probability distribution in the Fourier transformed domain (spatial or time domain) that is itself a power law. Exploiting this general feature, Cuomo *et al.* (1999) showed that the probability of finding a clear hole of linear size greater than L scales as a power of L itself with a scaling exponent close to 2. This analysis was performed on the basis of AVHRR imagery and the above scaling law was shown to hold in the range of scale 1000–100 000 m. The main aim of this Letter is to show that the same law may be extended down to a few metres. This extension has been obtained on the basis of AVNIR imagery of scattered clouds. AVNIR (Advanced Visible and Near Infrared Radiometer) is an imager that has flown on board of ADEOS (Advanced Earth Observing Satellite) from August 1996 to June 1997. The imager has four spectral bands, three of which are in the visible region (0.42–0.50 μm, 0.52–0.60 μm, 0.61–0.69 μm) and one in the near-infrared (0.76–0.89 μm), with 16 m of spatial resolution at nadir. In addition, AVNIR has a Panchromatic band (0.52–0.69 μm), whose spatial resolution is twice as fine (8 m). However, this band has not been used in this work.

2. Data and methods

Our analysis relies on two sectors of ADEOS/AVNIR scene which has been recorded over Japan (see figure 1). Since we are not interested in large and compact cloudy, or clear areas where we cannot find holes, the imagery have been selected in order to reproduce a sufficiently large variety of broken cloud systems through which it is possible to assess some underlying law governing the frequency of holes of a given size. AVNIR binary cloud masks have been computed at the full spatial resolution using only the traditional threshold tests on the reflectance in the visible and near-infrared channels. The scene has been then rendered to a lower spatial resolution and co-located with the original image, a procedure which allows us to compute a cloud mask for the new image. This process is similar to the usual procedure used, e.g. for co-locating HIRS (High Infrared Resolution Sounder) and AVHRR scenes to determine the cloud fraction inside each HIRS pixel. We may thus define a cloud mask C_L for the AVNIR low spatial resolution image, where C_L may assume the values ranging from 0 to 100, corresponding to a complete overcast and clear sky situation, respectively. By rendering the original scene at various L spatial resolutions, we may simulate radiometer with a spatial resolution ranging from $L_{\min}$ to $L_{\max}$. For the work here reported $L_{\min} = 0.48$ m, whereas $L_{\max} = 1500$ m which is approximately equal to the AVHRR spatial resolution.

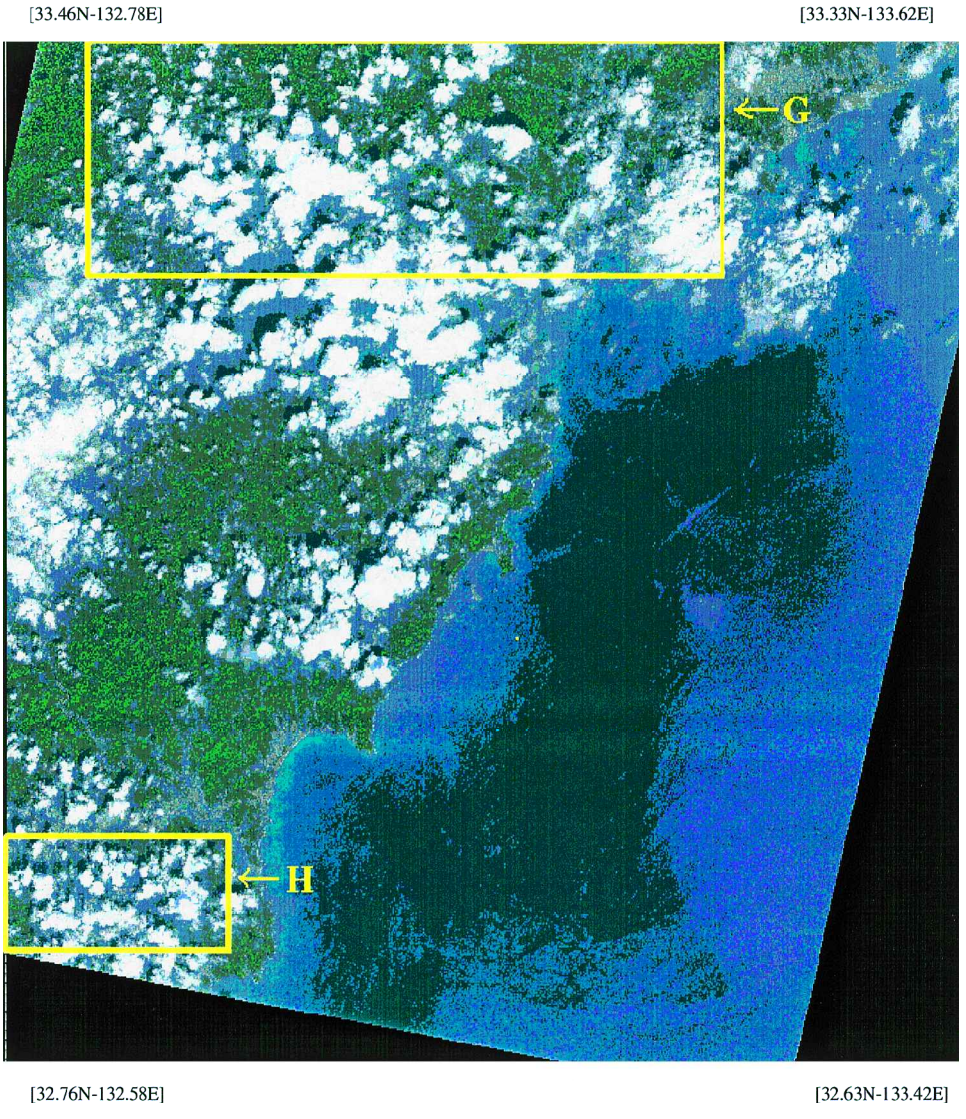

Figure 1. The AVNIR scene and the two sectors that have been analysed in this Letter (the scene size: 5000 pixels × 5000 pixels, RGB composition of channels 1, 2, 3). Geographic location is indicated by latitude and longitude at the corners. G: 2 September 1996, 02:09 GMT, 3300 pixels, 1140 lines. H: 2 September 1996, 02:09 GMT, 1162 pixels, 540 lines.

In practice, the process of rendering the original image at a lower spatial resolution is accomplished by covering the original image with square boxes (simulating the new field-of-view (FOV) of linear size $L/\Delta x = 96, 48, 24, 12, 6, 3$ AVNIR pixels, with $\Delta x = 16$ m being the linear size of the AVNIR pixel. Using this approach and these series of doubling linear FOV sizes, each simulated FOV of linear size L, is completely contained inside the one corresponding to the immediately lower linear spatial resolution, and at the same time, the FOV's number increase, inside the same area, by four times when L moves one position in the set (96, 48, 24, 12, 6, 3).

3. Clear area distribution

For the work here presented a given FOV or pixel of size L is flagged clear if $C_L = 95\%$ or more. Then, we define the Clearness Index $N_c(L)$ according to:

$$N_c(L) = \frac{\text{Clear FOV number of size } L}{\text{Total number of FOV of size } L} \quad (1)$$

which gives the fraction, over the scene, of clear FOVs when the linear size is equal to L. Figure 2 shows $N_c(L)$ for the two sectors which have been examined in this work. It is possible to appreciate the growth of clear pixels as L becomes small.

To model this kind of behaviour, we have computed the cumulative distribution $P(L)$ which is defined as the frequency of clear FOVs whose linear dimension is greater than L. This distribution has been obtained by averaging over the two sectors.

From figure 3, which shows $P(L)$ obtained by combining our previous results for

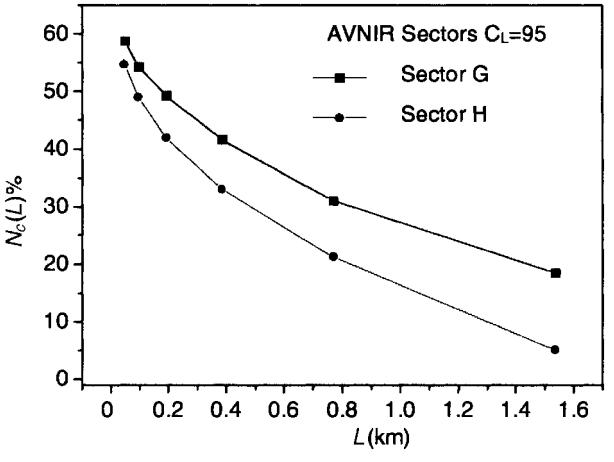

Figure 2. $N_c(L)$ as a function of L for the two sectors of the AVNIR scene.

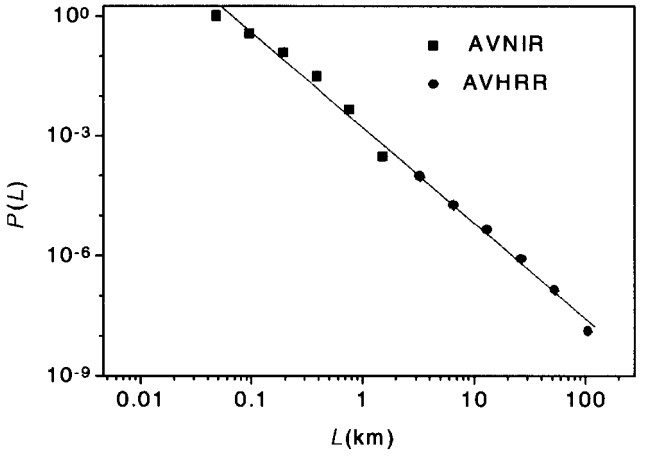

Figure 3. Cumulative distribution $P(L)$ obtained by AVNIR analysis combined with previous results obtained on the basis of AVHRR data. The slope value is 2.4 and the coefficient of determination is $(R^2) = 0.99$.

the AVHRR sensor (Cuomo *et al.* 1999) and AVNIR results, it is possible to appreciate the substantial continuity of $P(L)$ moving from the larger to the shorter length scales. The log-log plot shown in figure 3 evidences an underlying power law

$$P(L) \sim L^{-D} \tag{2}$$

Moreover, the scaling exponent D serves its value around 2. It should be stressed that AVHRR imagery referred to cloud systems over the Atlantic Ocean, whereas AVNIR scene was recorded over land and in a different location. Our findings highlight that the power law $P(L) = L^{-D}$ has to be linked to the presence of a universal law governing cloud morphology, intimately related to the physical processes of cloud-genesis and independent of season and latitude.

4. Conclusions

Our analysis brings new evidence that scale invariance in broken clouds seems to hold down to a few metres. An important aspect of this behaviour is that the probability of achieving more and better distributed clear soundings simply improves by: (1) reducing the size of FOV (the smaller, the better); (2) increasing the sampling density for a given target or sounding area which would be done by improving the FOV array of the sensor, e.g., 3×3 FOV array instead of the usual 2×2 geometry. This result has to be, of course, compromised with other technological constraints, and in this context it provides a mathematical model to trade-off between costs and relative density of clear soundings.

Acknowledgments

Work supported by the Italian National Space Agency (ASI).

References

Cuomo, V., Pietrapertosa, C., Serio, C., and Tramutoli, V., 1999, Assessing the impact of cloud morphology on infrared sounder scan geometry. International Journal of Remote Sensing, **20**, 169–181.

Duroure C., and Guillemet, B., 1990, Analyze des htrognit spatiales des stratocumulus et cumulus. Atmospheric Research, **25**, 331–350.

Lovejoy, S., 1982, Area-perimeter relation for rain and cloud areas. Science, **216**, 185–187.

Lovejoy, S., Schertzer, D., and Tsonis, A. A., 1987, Functional box-counting and multiple elliptical dimension in rain. Science, **225**, 1036–1038.

Mandelbrot, B. B., 1982, The Fractal Geometry of Nature (San Francisco: Freeman).

Parker, L., Welch, R. M., and Musil, D. J., 1986, Analysis of spatial inhomogeneities in cumulus clouds using high spatial resolution. Landsat data. Journal of Climate and Applied Meteorology, **25**, 1301–1314.

Serio, C., and Tramutoli, V., 1995, Scaling laws in baroclinic instabilities. Fractals, **3**, 297–314.

van der Ziel, A., 1950, On the noise spectra of semi-conductor noise and of flicker effect. Physica, **16**, 359–368.

Weger, R. C., Lee, J., Zhu, T., and Welch, R. M., 1992, Clustering, randomness, and regularity in cloud fields. 1. Theoretical considerations. Journal of Geophysical Research, **97**, 20 519–20 536.

Weger, R. C., Lee, J., and Welch, R. M., 1993, Clustering, randomness, and regularity in cloud fields: 1. The nature and distribution of clusters. Journal of Geophysical Research, **98**, 18 449–18 463.

YANO, J. I., and TACKEUCHI, Y., 1987, The self-similarity of horizontal cloud pattern in the intertropical convergence zone. Journal of the Meteorological Society of Japan, **65**, 665–667.

ZHU, T., LEE, J., WEGER, R. C., and WELCH, R. M., 1992, Clustering, randomness, and regularity in cloud fields: 2. Cumulus cloud fields. Journal of Geophysical Research, **95**, 20 537–20 558.